Geophys. J. Int. (2009) **176,** 431–442 doi: 10.1111/j.1365-246X.2008.03975.x

Mapping offshore sedimentary structure using electromagnetic methods and terrain effects in marine magnetotelluric data

Steven Constable,[1] Kerry Key[2] and Lisl Lewis[3]

[1] *Scripps Institution of Oceanography, La Jolla, CA, USA. E-mail: sconstable@ucsd.edu*
[2] *Scripps Institution of Oceanography, La Jolla, CA, USA*
[3] *WesternGeco Oslo Technology Center, Oslo, Norway*

Accepted 2008 September 15. Received 2008 August 28; in original form 2007 November 25

SUMMARY

Marine magnetotelluric (MT) and marine controlled-source electromagnetic (CSEM) soundings can be used to study sedimentary structure offshore. In an example of this application, we collected MT and CSEM data in the 1-km deep water of the San Diego Trough, California. The Trough is a pull-apart basin and part of the complex Pacific/North American tectonic plate boundary, and is flanked by the Thirtymile Bank to the west and the Coronado Bank to the east. Our MT data are highly distorted by seafloor topography and the coast effect, which is largely 2-D and can be modelled using 2-D finite element codes. The distortion includes a strong (several orders of magnitude) static depression of TM mode resistivities (electric field perpendicular to structure), upward cusps in the TE mode resistivities (electric field parallel to structure) and negative TE mode phases. The depressed TM mode resistivity is a well-known consequence of galvanic interruption of coast-perpendicular electric fields. The TE mode distortion is an inductive effect associated with currents flowing along the edge of the deep ocean basins, steepening the magnetic field and even causing a phase reversal in the horizontal field used for MT impedance calculations (and thus generating negative phases). The land-side enhanced vertical magnetic field is well known as the geomagnetic coast effect, but the ocean-side consequences have been less well documented.

Although the MT data are dominated by coast effect and topographic distortion, inclusion of accurate bathymetry in the inversion model's finite element mesh allows the subseafloor geological structure to be recovered. This shows the Trough sediments to be about 3 km thick, bounded to the west by resistive basement, but to the east by conductive clastic sediments forming Coronado Bank. Amplitudes and phases of five frequencies of CSEM data (from 0.1 to 1.0 Hz) collected along the axis of the Trough are well fit with a simple, 1-D layered model, indicating that sediment resistivities increase with depth from 1.5 to 2.3 Ω-m and are no more than 3300 m thick, thinning to the north, in good agreement with the MT model. An existing density model generated by fitting surface and deep-towed gravity is in good agreement with the EM interpretations. In particular, combining sediment densities and CSEM resistivities allows us to estimate pore water conductivity and temperature, which follows a geothermal gradient of $25.4 \pm 8\,\mathrm{K\,km^{-1}}$.

Key words: Electrical properties; Magnetotelluric; Marine electromagnetics; Heat flow; Sedimentary basin processes.

1 INTRODUCTION

Electromagnetic (EM) geophysical methods are widely used to study the structure of sedimentary basins on land, in both academic and exploration contexts. Magnetotelluric (MT) sounding, in which the EM response to time variations in Earth's magnetic field is measured as a function of frequency and position, is the most commonly employed method (e.g. Vozoff 1972), but controlled-source electromagnetic (CSEM) soundings, where the response to a man-made source of energy is measured, are also sometimes used (e.g. Gomez-Trevino & Edwards 1983; Hördt *et al.* 1992). The early use of MT and CSEM methods in the marine environment concentrated on the study of the mantle and igneous rocks of the deep oceanic lithosphere (e.g. Filloux 1979; Cox 1980), rather than the sedimentary

basins of the continental margins, and entailed the deployment of small numbers of innovative, academically built, instruments for months at a time.

The recent commercialization of marine electromagnetic methods (e.g. Constable 2006) has required, and supported, improvements in marine EM instruments and methodology. Academic equipment designed for occasional deployment in deep water has evolved into more robust, reliable and compact instrumentation capable of rapid repeat deployments and of constituting large arrays of simultaneously recording instruments. Initially, development efforts focused on adapting CSEM receivers for use as MT recorders with better high-frequency response than their predecessors (Constable *et al.* 1998), with the objective of mapping structure in areas where the seismic method encounters strong reflections, such as evaporites, volcanics and carbonates. With the increasing interest in the use of CSEM methods for direct detection of hydrocarbons (e.g. Eidesmo *et al.* 2002; Constable & Srnka 2007), the MT recorder was used once again as a CSEM receiver, or a dual-use MT/CSEM instrument.

In this paper, we demonstrate that EM methods can effectively be used to map sedimentary structure in the offshore environment for purposes similar to those onshore. These may include basin reconnaissance, a low-cost alternative to the use of the seismic method, or as a component of an integrated geophysical transect or study. However, we also demonstrate that the offshore environment presents some unique challenges and opportunities that are seldom, if ever, encountered on land. In particular, seafloor topography and associated coastlines have a profound effect on MT transfer functions, and must be carefully included in the modelling and interpretation process if sensible results are to be obtained.

2 INSTRUMENTATION AND DATA COLLECTION

We collected both MT and CSEM data in the San Diego Trough (Fig. 1), a sediment-filled graben structure in the Catalina tectonic terrane of the California continental borderland (e.g. Teng & Gorsline 1991), bounded to the east by the Coronado Bank and the west by the Thirtymile Bank. The borderland is part of the extended plate boundary between the North American Plate and the Pacific Plate, and is cut by many northwest trending, dextral strike-slip faults which create pull-apart basins, of which the Trough is one example. With a sedimented seafloor in around 1000 m water

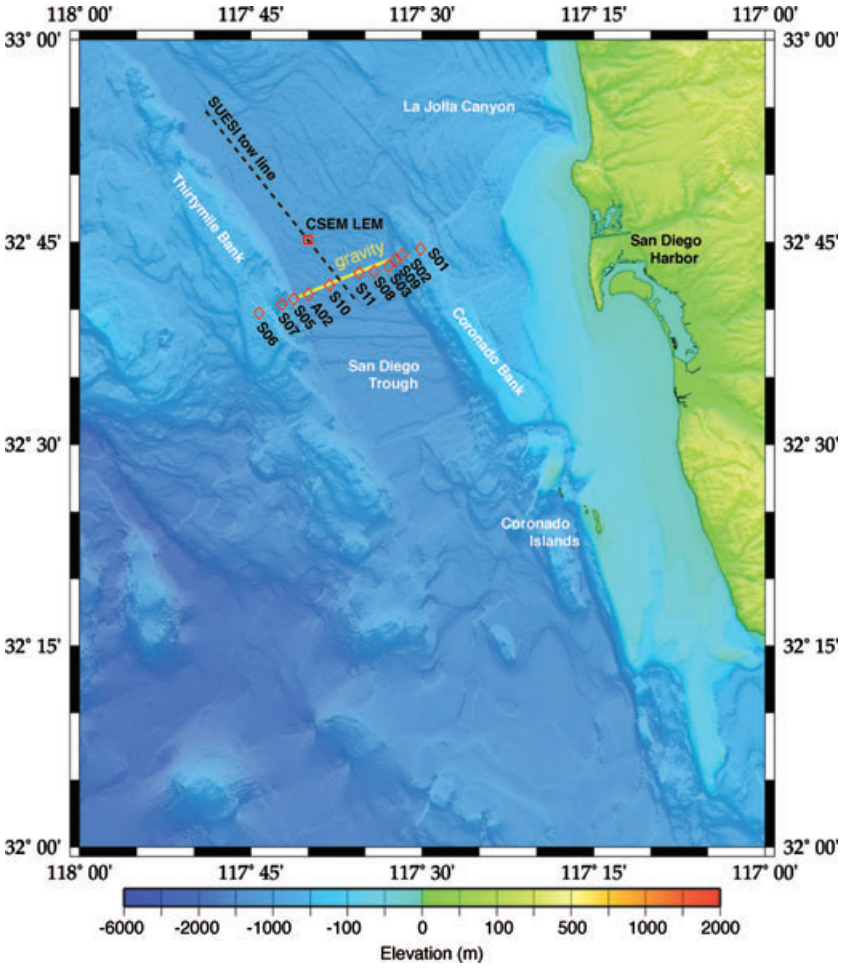

Figure 1. Regional map of the study area, showing MT stations (S06, S07, etc.), CSEM receiver ('LEM'), CSEM tow line and deep-towed gravity line (in yellow) of Ridgway & Zumberge (2002). Also shown are the main structural features of the area. The San Diego Trough is a 10-km wide, 1000-m deep sediment-filled graben bounded by the Thirtymile Bank to the west and the Coronado Bank to the east. The flat, sedimented seafloor, combined with the close proximity to San Diego harbour, makes the Trough a convenient place to develop marine instrumentation. Bathymetric map courtesy of the National Geophysical Data Center.

depth, the Trough presents a seafloor morphology and geology similar to those of interest to the offshore exploration industry (sans hydrocarbons), a fact which motivated and helped fund the studies presented here.

The proximity of the San Diego Trough to Scripps Institution of Oceanography (SIO) makes it a convenient place to test marine instrumentation being developed by SIO and collaborative partners. In this project, we collected marine MT data during three field trials carried out in 2003 and 2004 (Lewis 2005) as part of a study to test and evaluate a third-generation ('Mark III') CSEM/MT recorder. This instrument incorporates numerous improvements over the 'Mark II' instrument originally described by Constable *et al.* (1998), which include an increased number of data channels (from 4 to 8), replacement of disc drives with compact flash cards, expanded digitization from 16 to 24 bits, an ethernet interface to download data through the instrument pressure case, increased dynamic range by lowering the gain of the amplifiers, a vertical electric field capability, replacing the commercial magnetic sensors with a lighter, lower power version of our own design, adding recording electronic compass/tiltmeters and incorporating a glass stray-line buoy with integrated recovery light, GPS location and radio modem. Many of these features have been since retrofitted to the Mark II instruments still in use. The 'Mark I' instrument, now retired, is described by Constable & Cox (1996). As part of a later, separate project in 2006 we also collected CSEM data in the same area during a test of a CSEM transmitter.

To provide the opportunity to carry out joint interpretation with other geophysical data, we positioned the MT sites along the deep-towed gravity line of Ridgway & Zumberge (2002), which conveniently cuts across the Trough in a way that facilitates 2-D modelling and interpretation (Fig. 1). There were several aspects of the local geology that Ridgway and Zumberge were attempting to address with their experiment. Estimates of sediment thickness for the Trough vary; seismic reflection interpreted by Teng & Gorsline (1991) gives 2.0 km while a seismic refraction experiment of Shor *et al.* (1976) gave 3.0 km—the deep-towed gravity work implied 3.4 km. There is also some doubt as to whether the Coronado Bank is made up of sediments or basement rocks. Finally, the gravity study was designed to detect any density contrast across the San Diego Trough Fault, which, as implied by its name, runs almost exactly along the centre of the Trough.

3 CONTROLLED-SOURCE EM DATA

During an experiment in 2006, we deployed a sensitive EM receiver about 7 km northwest of the MT line. The receiver was a long-wire EM (LEM) instrument of the type originally described by Webb *et al.* (1985), but comprising a Mark III electric field recorder with a 200 m receiver antenna oriented along the axis of the Trough. Our deep-towed EM transmitter (SUESI—Scripps Undersea Electromagnetic Source Instrument) is a more modern version of the instrument described by Constable & Cox (1996) and was 'flown' 90 m above the seafloor along the centre of the Trough. The transmitter antenna was a neutrally buoyant horizontal electric dipole 200 m long, and the output current during this part of the experiment was a 380-A zero to peak square wave, to give a dipole moment of 96.8 kA m at the fundamental frequency. The output waveform cycled through 2 min of a 0.1 Hz square wave, 2 min of 1 Hz square wave and 1 min of 10 Hz square wave, although the 10-Hz data proved to be too high in frequency to be useful. Processing consisted of least-squares fitting of harmonics over each 2-min transmission window and averaging over two successive transmission cycles. Thus, the duty cycle for the data shown in Fig. 2 is 4 min transmission every 10 min. Tow speed was about 1.5 knots ($0.8\,\mathrm{m\,s^{-1}}$), so data are spaced about 500 m apart, with negative ranges plotted when the transmitter is southeast of the receiver. The phase convention is that phase lags are plotted as negative numbers.

The CSEM data were initially modelled using the 1-D code of Flosadottir & Constable (1996), and simple trial and error modelling using three layers (two sedimentary layers over resistive basement at a depth of 2800 m for the southern part of the tow and 2400 m for the northern half) produces a qualitatively adequate fit to the data. It is easy to see the effect of basement rocks in the phase data; the larger skin depth in the resistive rocks produces a much smaller phase shift over a given distance and thus a levelling of the slope of the phase versus offset curves. The range at which the change in slope occurs, about 7 km for southern transmissions and 5 km for northern transmissions, is controlled by basement depth. Two sedimentary layers of slightly differing resistivity are required to match more subtle changes in slope at shorter offsets, with the top layer of about 1000 m thickness. This correlates with a density change at a depth of 950 m observed by Ridgway & Zumberge (2002).

More rigorous interpretation of the CSEM data using inversion schemes requires a quantified misfit measure. The statistical noise in these data is around $10^{-15}\,\mathrm{V\,A^{-1}\,m^{-2}}$, which produces meaningless (i.e. too small) error bars when amplitudes are above about $10^{-13}\,\mathrm{V\,A^{-1}m^{-2}}$. Unless one is close to the statistical noise limit, errors are determined by instrument calibration, navigation and orientation of the transmitter, error in transmitter output and height, etc. Based on practical estimates of these, we assign a minimum error floor of 5 per cent of amplitude (which corresponds to 3° in phase) for data above the statistical noise threshold, recognizing that these sources of error are likely to be systematic rather than purely random. The noise threshold is frequency-dependent, decreasing from $5 \times 10^{-15}\,\mathrm{V\,A^{-1}\,m^{-2}}$ at 0.1 Hz to $5 \times 10^{-16}\,\mathrm{V\,A^{-1}\,m^{-2}}$ at 1 Hz.

We continue with the 1-D assumption and carry out Occam inversions (Constable *et al.* 1987) of the data. The assumption of 1-D structure is a pragmatic choice associated with the interpretation of a single site, but is fairly secure; the MT model (below) is quite uniform in this region, and indicates that the sediments are four times wider (about 10 km) than they are deep (2–3 km). A transmitter test during the deployment of station S10, reported by Constable & Weiss (2005), produced poorer quality data but a similar result (2350 m of 1.9 Ω-m sediment over resistive basement). Finally, the agreement across five frequencies, having peak sensitivity at different depths, supports the idea that the seafloor has a simple structure.

Recent work has shown that the electrical conductivity structure of the sea water layer must be included in the modelling to obtain accurate results, but the Flosadottir and Constable code does not easily allow this. Consequently, for inversions we used the code of Key (in press), and included a 22-layer water conductivity profile in the model, derived from values measured by instrumentation on the transmitter during lowering and recovering. Total water depth is 1140 m. Rather than carrying out fully unconstrained smooth inversions of the data, we use the inversions specifically to address the reliability of the sediment resistivity estimates and the depth to resistive basement. Thus, we fix the top sedimentary layer at thickness of 950 m for direct comparison with the gravity model of Ridgway & Zumberge (2002), and systematically vary the thickness of the next sedimentary layer until an acceptable misfit is no longer obtainable. The best root-mean-square (rms) misfit from this class of model is 1.3 (southern tow) or 1.4 (northern tow), and so we set

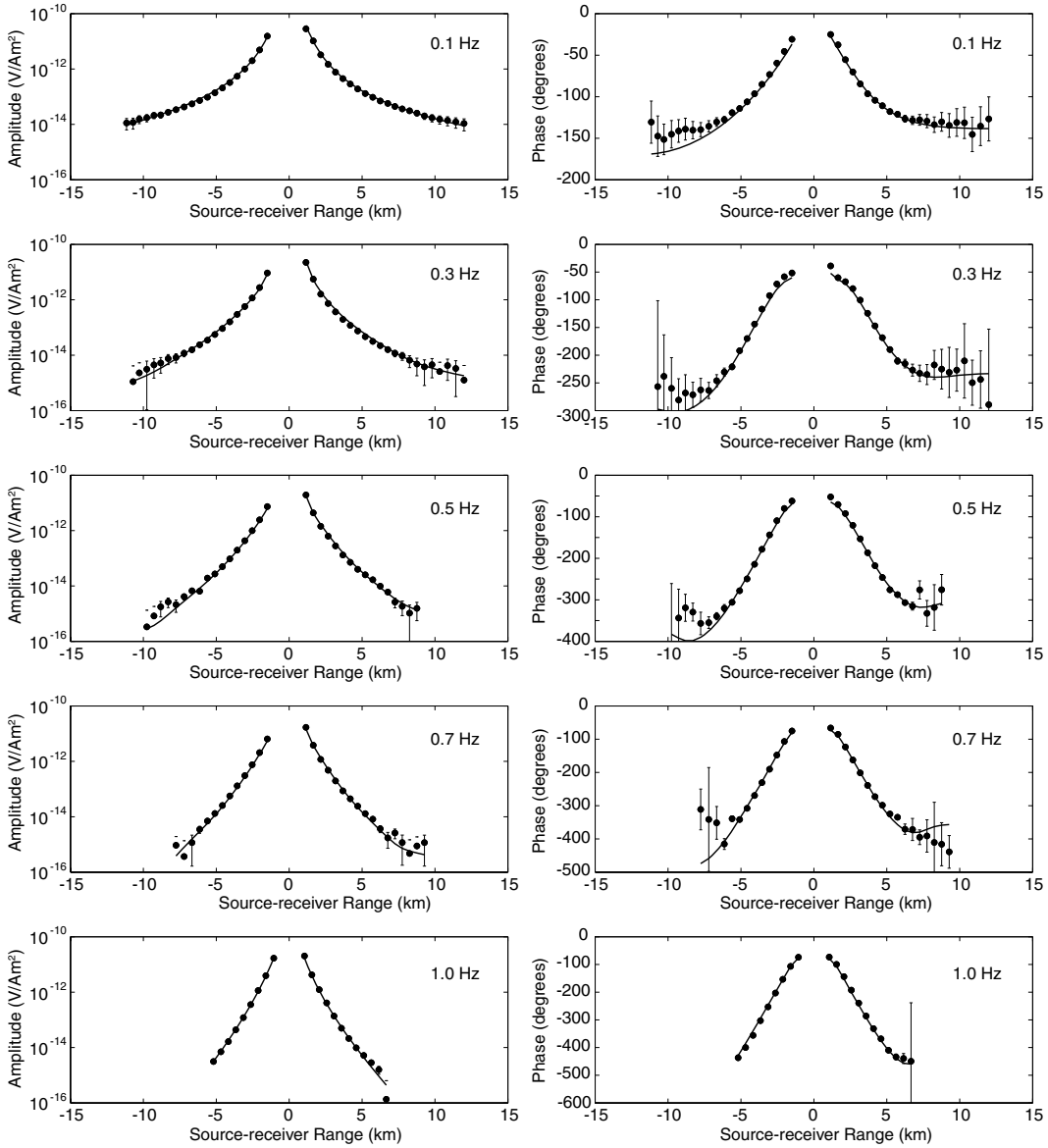

Figure 2. Controlled-source EM data collected along the axis of the San Diego Trough (see Fig. 1 for location). Amplitude (left-hand panels) and phase (right-hand panels) over 4 min of stacking are shown versus transmitter position along the tow line (horizontal axis, north positive) for the first four 0.1 Hz square wave harmonics and 1 Hz fundamental. Solid lines are the response of the rms 1.6 model shown in Fig. 3 having the maximum basement depth. The receiver instrument is at 0 km.

the level of acceptable fit at rms 1.6, or 8 per cent in amplitude. Because phase wraps beyond 360° at the higher frequencies, we carry out the inversions on the real and imaginary components of the data, rather than amplitude and phase, assigning equal absolute errors from amplitudes to both components.

Fig. 3 shows the results of the inversion study. All resistivities are free to vary except those of the sea water. For the southern tow, acceptable fits cannot be obtained if the basement is placed below 4400 m (about 3300 m below seafloor), which places an upper bound on depth. Shallower basement can be accommodated by reducing the resistivity contrast. For the northern tow, maximum basement depth is 3600 m (about 2500 m below seafloor). The Trough sediments are thought to thin to the north, so this is consistent with prior understanding as well as the forward model studies.

The sediment resistivity varies very little as the depth to basement is changed. The 950 m upper layer varies from 1.49 to 1.52 Ω-m in the south and 1.43 to 1.48 Ω-m in the north. The deeper sediments vary from 2.14 to 2.32 Ω-m in the south and 2.04 to 2.58 Ω-m in the north. The basement resistivity is undetermined; it must be at least an order of magnitude more resistive than the sediments, but can be made arbitrarily high.

4 MAGNETOTELLURIC DATA AND SEAFLOOR TOPOGRAPHY

The MT data are shown in Fig. 4. The time-series were 5 d long (except for stations S10 and S11 which were 48 hr) and processed using the multistation code of Egbert (1997). We find that the multiple station noise estimation and robust down weighting used in this code are sufficient to obtain good quality MT responses in local seafloor MT arrays without the need for a far-away reference site.

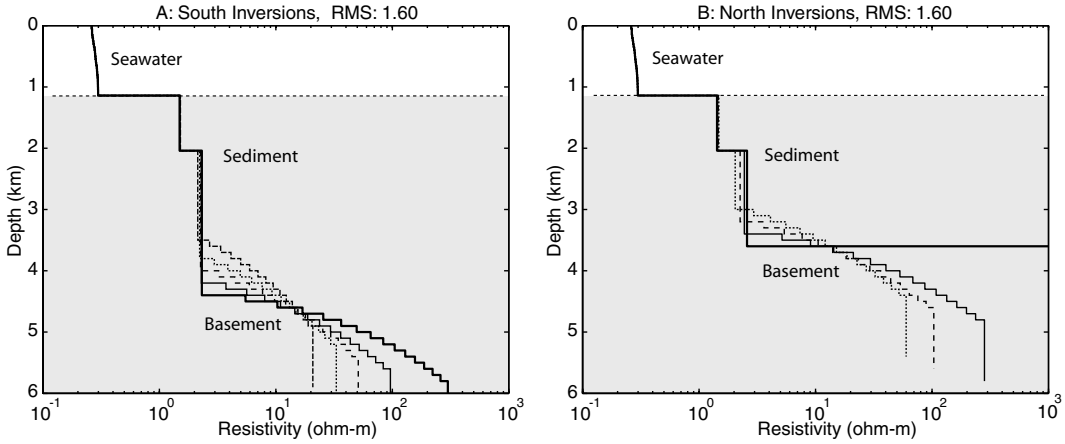

Figure 3. Occam inversions of data shown in Fig. 2 for various basement depths, all fitting to rms 1.6, for the southern transmitter tow (A) and northern tow (B). Sea water resistivity structure is fixed, but all other resistivities can vary. However, the thickness of the two sedimentary layers are fixed in each inversion. The heavy line shows the preferred model with the deepest basement, and generates the responses shown in Fig. 2.

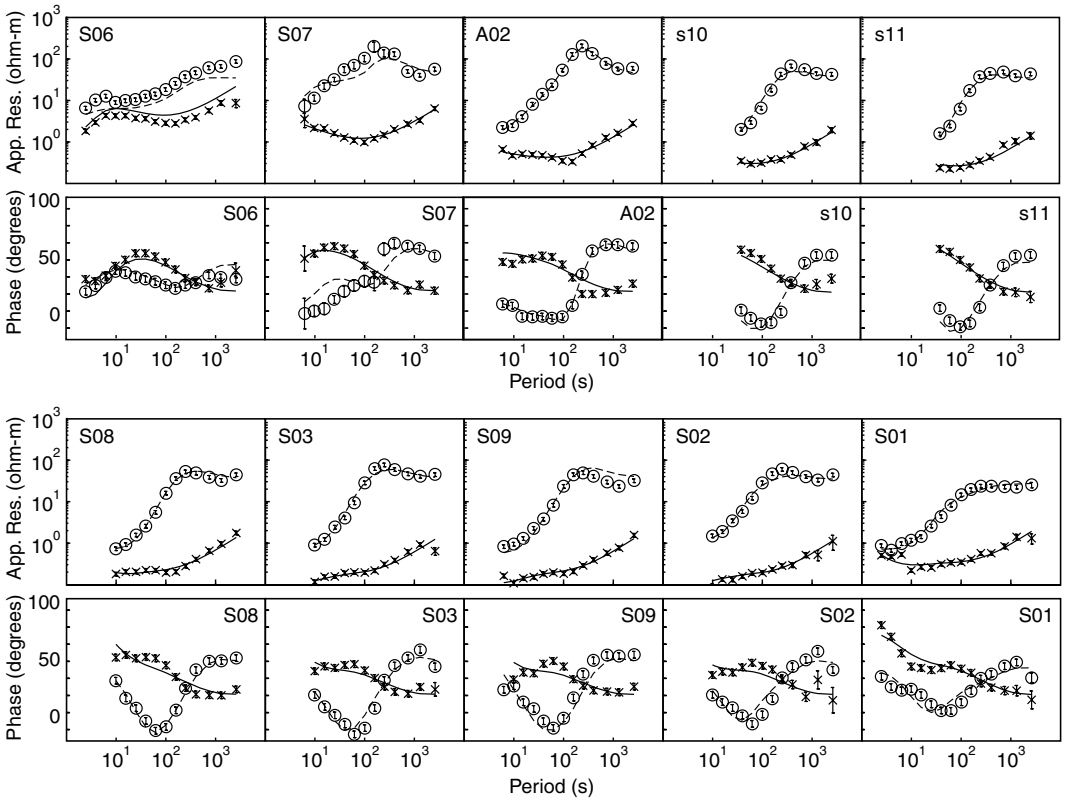

Figure 4. MT data collected across the San Diego Trough, rotated to the impedance maximum, which is parallel to the strike of the coastline and Trough. Station positions are given in Fig. 1. Strike-parallel electric field (TE mode) is shown as circles, and strike-perpendicular electric field (TM mode) as ×. Lines are forward responses from the inverse model shown in Fig. 10 (broken lines for TE mode, solid lines for TM mode).

Most of the MT responses have impedance skews (Swift 1986) less than 0.2 and dominant off-diagonal terms in the impedance matrix, suggesting they are compatible with 2-D structure and induction (see e.g. Figs 5 and 6). The exception is site S05, which is located on a slump complex at the base of the Thirtymile bank and has skews in the range 0.2–0.4, and we have omitted this site from further 2-D interpretation. MT responses were rotated to maximize the off-diagonal impedances. This is consistent with the dominating effect of 2-D induction associated with the Trough topography and with the 2-D interpretation presented below, and agreed with the independent estimates of orientation, which were of variable quality because the internal recording compasses were often contaminated by fields from the magnetic sensors and batteries (this has since motivated the use of external compasses for orientation). Some instrument orientations were estimated by correlating fields against land references of known orientation. No decomposition was applied (we explain this below). Sites on the shallower flanks of the Trough (S06 and S01) have reasonably good data to periods as short as 1 s. The sites on the floor of the Trough, in about 1100 m water, have good data to at least 10 s period, except for S10 and S11,

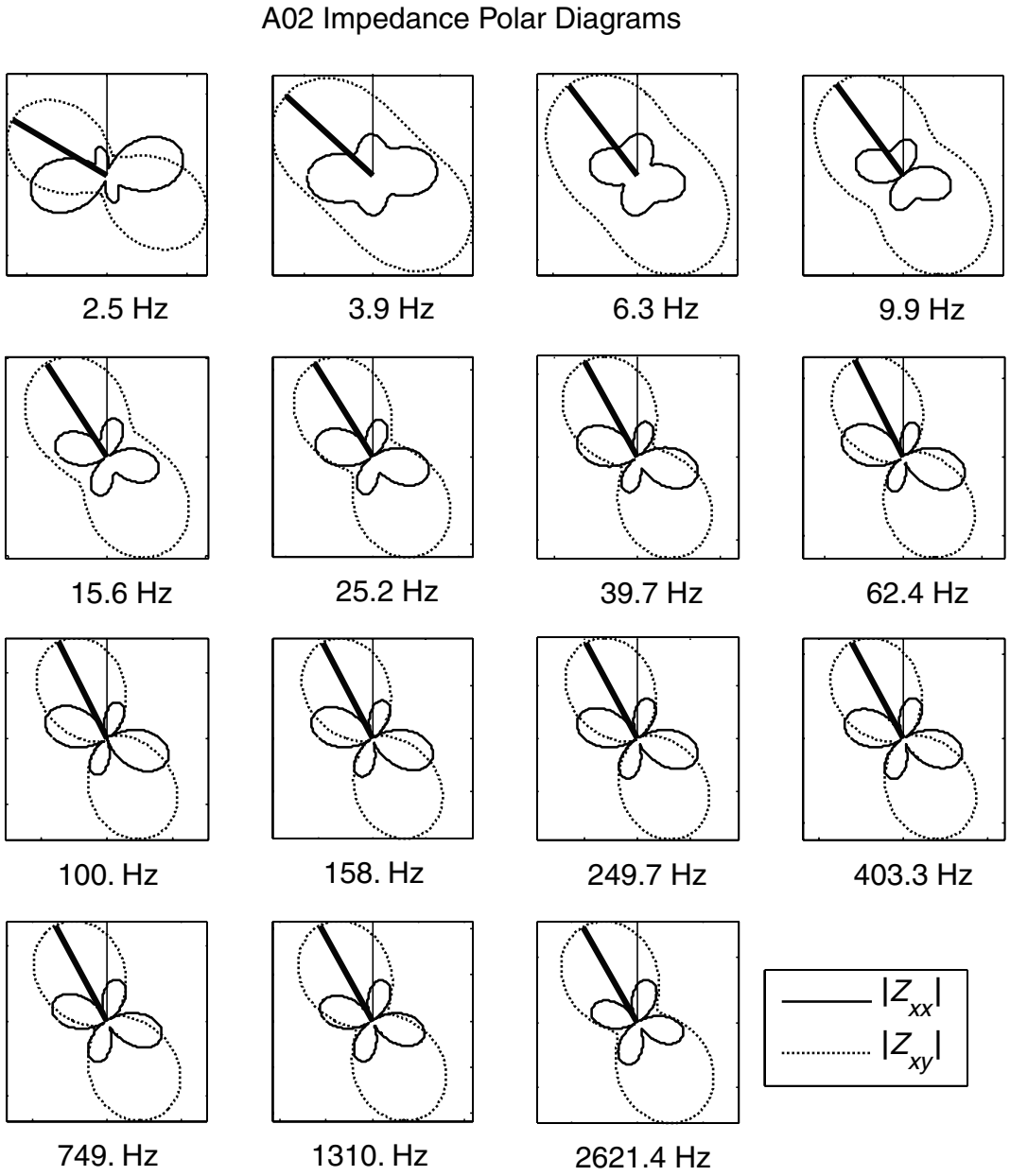

Figure 5. Impedance polar diagrams for MT site A02, in geographic coordinates (north upwards). The off-diagonal components, represented by the broken lines, show a strong 2-D response except at the shortest period, with a stable direction of maximum electric field aligned along the axis of the Trough.

which were deployed for a much shorter time and have lost about half a decade at the short period end of the response curves. The long period limit does not seem to be associated with deployment time, and good data to several thousand seconds were obtained in almost all cases. The long period limitation is probably caused by the use of magnetic coils, which have a $\mathrm{d}B/\mathrm{d}t$ response which rolls off like a one-pole filter at long periods, and capacitive coupling of the electric sensors, which has a similar effect.

The MT responses exhibit behaviour that would be considered highly unusual, if not pathological, for land MT curves, but which we have learnt to recognize as characteristic of 2-D topography and coastlines. We see extreme anisotropy, up to four orders of magnitude, between the TE (electric field parallel to structure) and TM modes (electric fields perpendicular to structure), with the TM resistivities depressed to unphysically small values (as low as 0.1 Ω-m in this case). This behaviour has been fairly well understood for nearly three decades as the ocean side of the coast effect, caused by galvanic distortion as the coast-perpendicular electric fields intercept resistive seafloor topography and the coastline itself (Cox 1980; Ranganayaki & Madden 1980). The TE mode behaviour is somewhat more unusual. The resistivities are characterized by a cusp at around 100 s period, with a corresponding minimum in phase which goes negative for several sites by as much as 10°. These are inductive effects associated with electric currents flowing parallel to the coast, and although this has long been understood to be associated with the vertical magnetic field behaviour of the land-side coast effect (e.g. Fischer 1979), the seaward side of this phenomenon has gone largely unreported. Thus, before we present the inversion results of our data, it is instructive to examine the effect of terrain in the absence of seafloor conductivity structure.

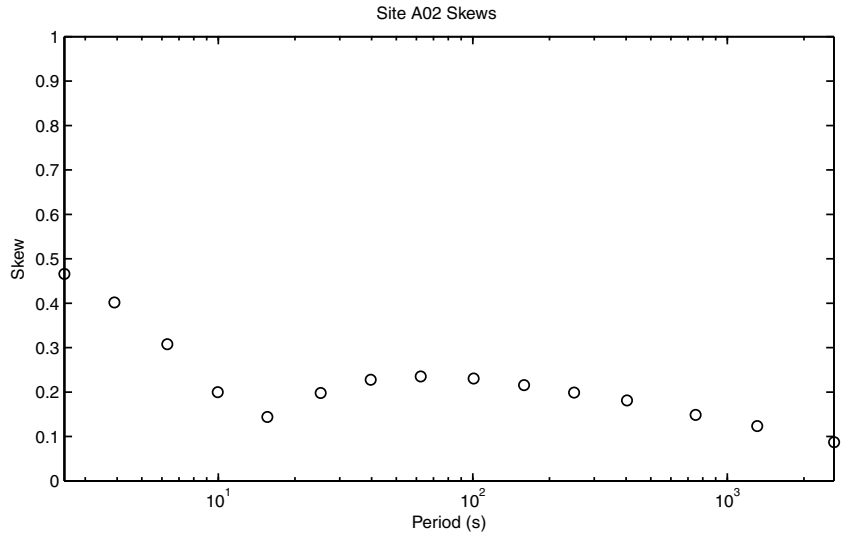

Figure 6. Skews for MT site A02 are below 0.2 except at the shortest periods, which supports the assumption of responses dominated by 2-D structure.

Modelling seafloor topography places severe demands on computational algorithms because the model contains significant conductivity contrasts very close to the observation sites, where fields need to be well predicted. Bathymetry can be directly included in both finite difference (FD) and finite element (FE) models. With FD methods, which have advantages in computation and algorithmic simplicity, the depth variations must be handled using the 'stair-case' method, whereby rectangular conductivity cells approximate the sloping seafloor as sequences of stair steps with variable height and width. The resulting grids can be very large and highly variable in cell dimension. Baba & Seama (2002) present a variation of the FD method where the bathymetry is transformed into changes in conductivity and magnetic permeability in FD cells above and below a flat seafloor, resulting in a smaller and more uniform grid. However, it is not clear that this method would work for the Trough since the depth variations are of the same order as the target sedimentary basin depth, and the relatively high-frequency responses impose greater demands on the approximations used. Instead, we use the FE method, which offers the advantage of using triangular elements which can closely conform to the seafloor, at the cost of greater algorithmic complexity. For the inversions (below), we use the rectilinear FE code of Wannamaker *et al.* (1987), but for the forward solutions, we use the MARE2DMT modelling code of Key & Weiss (2006), which uses unstructured triangular meshes and an adaptive refinement algorithm that allows the seafloor to be automatically meshed as finely as required for accurate solutions. Fig. 7 shows the responses computed by MARE2DMT for a site placed in the Trough at the same location as the real site S03, and for uniform seafloor resistivities between 1 and 1000 Ω-m.

Starting with the TM mode, we see that phase is largely unaffected, except for some short-period inductive behaviour for the 100 Ω-m seafloor, but the effect of the bathymetry and coastline depresses apparent resistivity for seafloor resistivities higher than 10 Ω-m, to the point where the response of the 1000 Ω-m seafloor is lowered to around 1 Ω-m. The largely frequency-independent shift of the apparent resistivities and the lack of phase corruption is characteristic of galvanic distortion and is similar to static shift effects in land MT studies. However, on land static shift is associated with small scale structure local to the electrode arrays, while here this 'static' distortion is a result of large scale topography and coastlines. The 2-D model was constructed from a bathymetry profile running from the deep ocean beyond the continental shelf, across the survey line in the Trough, and extending 20 km east to the California coastline. In particular, it was found that inclusion of the coastline, as well as local bathymetry, was essential for obtaining the large split between TE and TM mode responses. Indeed, if the underlying crust and mantle are resistive, these galvanic effects can propagate laterally for very large distances, which led Heinson & Constable (1992) to conclude that no part of the global ocean basin is immune from this part of the coast effect.

The TE mode is more complicated, with inductive effects in both resistivity and phase which are far from frequency-independent. At short periods, the apparent resistivity is depressed, but with a sharp upward cusp in resistivity developing around 100 s period for a 100 Ω-m seafloor. The depressed resistivities and cusp are associated with anomalous phases, which even go negative. For the 100 Ω-m seafloor, the phases are modestly negative, quite similar to the actual data, but for higher resistivity (1000 Ω-m), phases go extremely negative and even exceed -180° and wrap. We have seen such wrapping in real data near the continental slope, and have observed that the period at which phase goes negative or wraps is only weakly dependent on seafloor resistivity, which suggests the phenomenon is dependent on the geometry of the bathymetry and MT site location.

Our modelling shows that the strange behaviour of the TE mode is caused by the same phenomenon that produces the classical landside coast effect, namely anomalous vertical magnetic fields caused by induced electric currents flowing along the edge of the ocean (e.g. Fischer 1979). In Fig. 8, we have contoured the TE electric field at a period of 100 s for a Trough of uniform 100 Ω-m seafloor. These contours of constant electric field amplitude correspond to stream lines in the TE magnetic field. The vertical plane of the magnetic field curls around the lateral edge of a sheet of TE mode electric current flowing in the deeper parts of the ocean, lowering the horizontal component on the seafloor below the overlying current sheet, which, combined with enhanced electric fields, increases apparent resistivity. When the magnetic field actually goes through vertical, the denominator in the apparent resistivity formula goes to zero, causing the cusp in resistivity, and the horizontal magnetic field then reverses to create the negative phases.

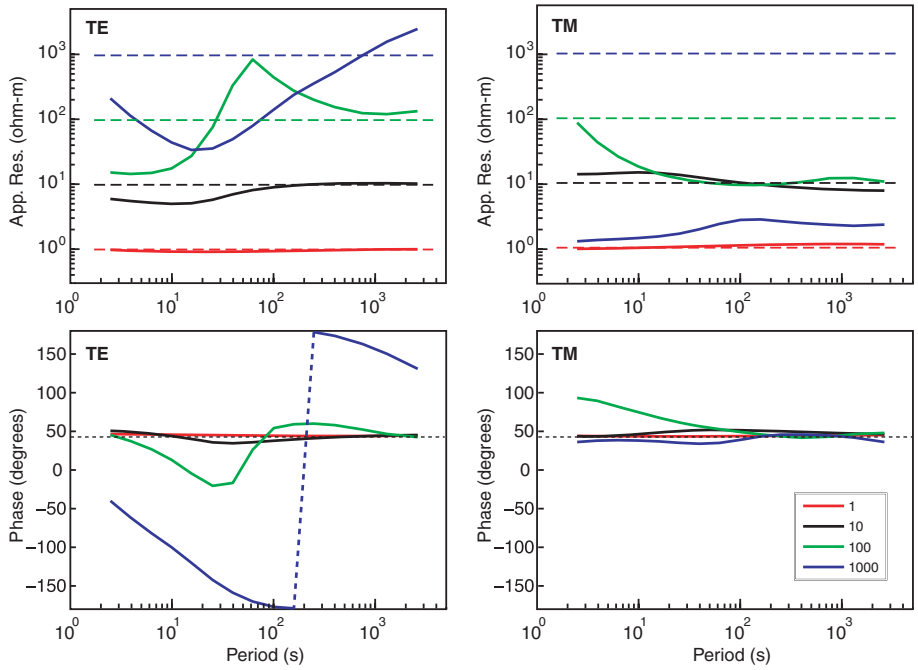

Figure 7. Forward model response for site S03 using the forward code of Key & Weiss (2006) to model bathymetry for various uniform seafloor resisitivities (1 Ω-m shown in red to 1000 Ω-m shown in blue). The broken horizontal lines show the apparent resistivities which would be observed in the absence of bathymetry (the phase for such a flat seafloor would always be 45°). The TE mode (electric field parallel to structure) develops cusps in apparent resistivity and negative phases when the seafloor resistivity reaches 100 Ω-m, while the corresponding TM mode resistivities are suppressed by about an order of magnitude, with little distortion of phase. For 1000 Ω-m seafloor, the distortion is extreme in both modes.

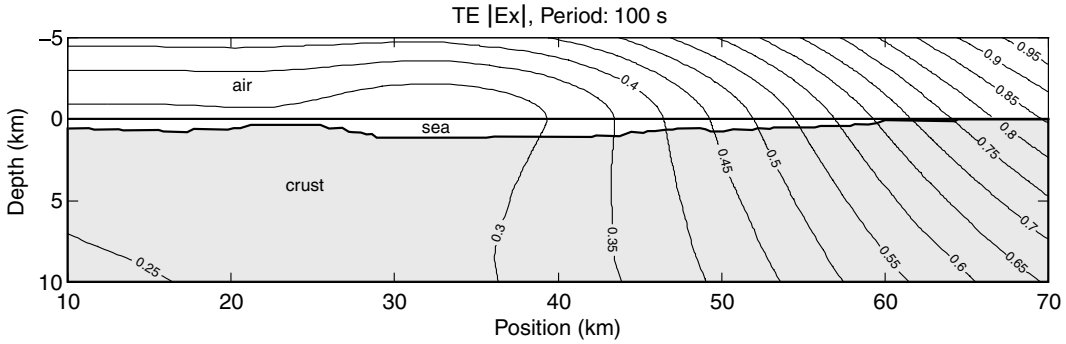

Figure 8. Contours of the magnitude of the TE electric field at a period of 100 s for a trough of uniform 100 Ω-m resistivity seafloor (units are relative). Such contours of constant electric field amplitude correspond to stream lines in the TE magnetic field, showing the steepening near the centre of the Trough associated with the apparent resistivity cusps and negative phases shown in Fig. 7. Contours return to horizontal at the left-hand and right-hand edges of the model (not shown), but do show the increased vertical component on the right-hand side associated with the classic land-side coast effect.

To summarize, the effect of coastlines and seafloor topography is to cause the TM mode response to saturate at long periods and lose sensitivity to seafloor resistivity, but the TE mode becomes very sensitive, especially in the phase. Although they considered a different structure, Schwalenberg & Edwards (2004) found similar effects for sinusoidal seafloor topography, where the TM mode experienced a galvanic distortion of apparent resistivity with almost no phase distortion, and the TE mode had large distortions in both amplitude and phase.

Comparison of the site S03 data in Fig. 4 and the 100 Ω-m responses in Fig. 7 shows that the structure of the resistivity and phase data are in large part explained by bathymetry and a uniform seafloor. This makes it very clear that to obtain more complicated geological structure (than a uniform seafloor), seafloor topography will have to be accurately computed as part of the inversion process. Although schemes exist to correct the data for bathymetry effects (e.g. Baba & Chave 2005), they are valid only for imaging upper-mantle structure where the bathymetry and mantle structure can be decoupled across the resistive lithosphere. Finally, we note that attempts to correct the data for static shifts using decomposition algorithms are guaranteed to undermine the ability to include, and account for, topography during the modelling and inversion process. Since seafloor sediments tend to be uniform in conductivity, and the high conductivity of sea water reduces galvanic effects from any near-seafloor conductivity contrasts that do exist, decomposition schemes, while clearly useful on land, are probably not normally necessary for marine MT studies.

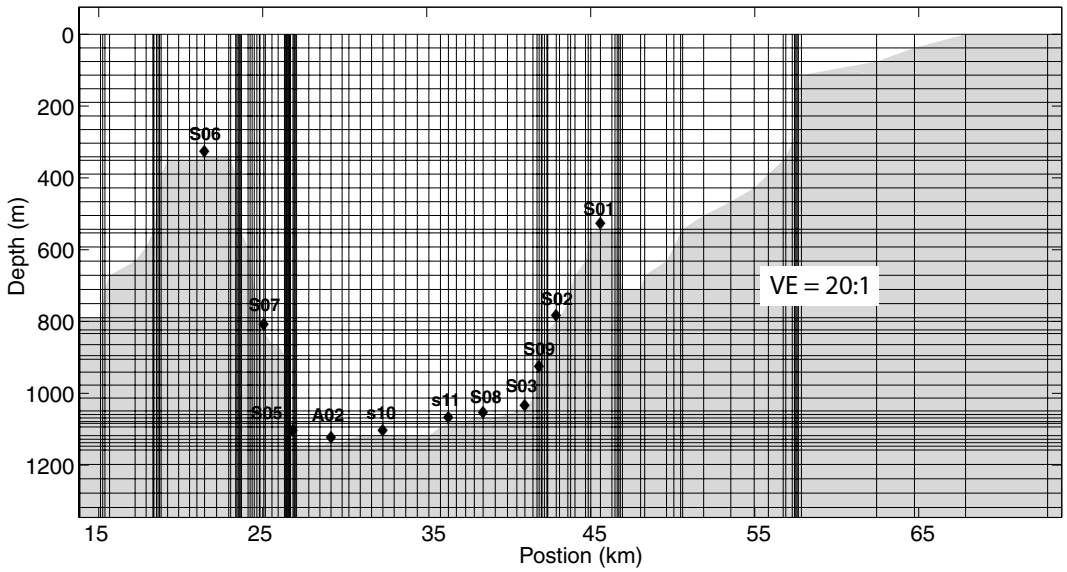

Figure 9. A subset of the finite element mesh used to invert our marine MT data using the OCCAM2DMT code of deGroot-Hedlin & Constable (1990). The mesh geometry associated with the forward code of Wannamaker *et al.* (1987) is rectilinear, but allows triangular subelements and tolerates elements with large aspect ratios. Sites are shown as diamonds and correspond to those shown in Fig. 1.

5 INVERSE MT MODELLING

We have not yet implemented the Key & Weiss (2006) code in an inverse MT algorithm, and so for inversions we use the OCCAM2DMT code of deGroot-Hedlin & Constable (1990), which uses the FE forward modelling code of Wannamaker *et al.* (1987). Although the Wannamaker code uses rectangular elements, and thus suffers from propagation of element size throughout the mesh, it does use triangular subelements which may be of large aspect ratio, making topographic meshes tractable.

However, generating a mesh which represents bathymetry reasonably well but which manages the rectangular element propagation is not particularly easy. We wrote a numerical scheme to do this automatically for given bathymetry and station locations, initially in FORTRAN and then later in MATLAB. The algorithm creates vertical nodes based primarily on station depths (stations need to be positioned on nodes), placing additional nodes in between to ensure a minimum vertical element size. It then places nodes in the horizontal direction to best track the bathymetry. Fig. 9 shows a section of the mesh which we used to invert the data. Even though vertically exaggerated, this figure provides some indication of the extreme topography we are dealing with. Fortunately, Trough topography is largely 2-D; 3-D inversion with bathymetry is not currently practical.

Fig. 10 shows the maximally smooth model (in the sense of minimum gradient) which fits the data set to rms 2.2 (the data error floor was set to 10 per cent in apparent resistivity). The fits of the MT model to the data are shown in Fig. 4. The fits are very good; in particular, the cusps in the TE mode resistivities and the negative phases are well represented in the model responses.

In the MT inversion, the sediments of the Trough form a conductive triangle (but note the vertical exaggeration) of around 1 Ω-m extending to a depth of about 4 km (from sea surface; 3 km below seafloor). Thirtymile Bank to the west is resistive at around 100 Ω-m, except for some shallow conductive structure. The upper 1 km of Coronado Bank to the east, however, is about as conductive as the Trough sediments. The model resistivities east of Coronado Bank are very high, around 1000 Ω-m, but this only represents bulk resistivity since we have no sites here and thus limited resolution (the model extends from the coastline to the east to the continental slope to the west).

We have overlain the MT resistivities on seismic data collected by the U.S. Geological Survey. We have also painted in the gravity model of Ridgway (1997), which, although constrained heavily by seismic data, suggests a low density core for the Coronado Bank and a depth to basement in the Trough of about 3.4 km. Finally, we have represented the southern CSEM model on the same colour scale as for the MT resistivities.

The MT model, taken alone, provides basic structural information of interest to a geologist or an explorationist. The sediments of the Trough are about 3 km thick and bounded to the west by the basement rocks of the Thirtymile Bank. To the east, the Coronado Bank does not form a resistive boundary to the Trough sediments, but appears to be also composed of porous clastic sediments. One could tighten up the estimate of sediment thickness either by forward model studies or sharp boundary inversion (e.g. Smith *et al.* 1999; deGroot-Hedlin & Constable 2004), but in this case we can not only validate the results from the MT study, but also provide tighter constraints on geology, using the other geophysical data.

The seismics provide a good indication of the western edge of the sediments, which the MT model tracks well. The gravity model also tracks this contact, but was based to some extent on the seismic results. The patch of lower resistivities on the flank of Thirtymile Bank corresponds to lower densities inferred, but not modelled, by Ridgway (1997). He observed that a uniform density of 2700 kg m^{-3} for Thirtymile Bank overpredicted the observed data and noted that dredged samples of the volcanics in this area had a broad range of densities. Legg & Kamerling (2003) inferred landsliding in this area based on the seismic evidence.

It is difficult to tell from the seismics alone what the geology of Coronado Bank is, but based on the gravity and inspection of proprietary seismic lines from industry, Ridgway chose a lower density for the Bank with a basement core at depth. The MT resistivities agree remarkably well with this interpretation. The patches of very

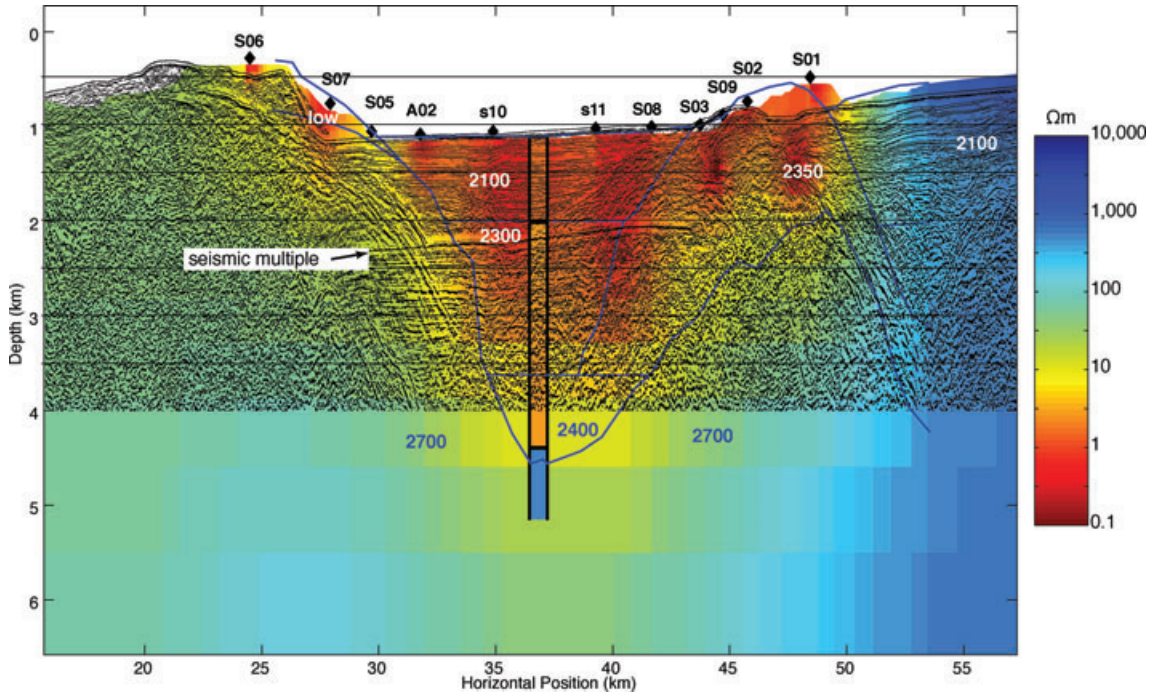

Figure 10. Inversion of MT data (colour pixel-plot) overlain on USGS seismic line 112 (black pattern). Also shown as blue lines and densities (blue and white numbers, kg m^{-3}) is the model derived from surface and deep-towed gravity by Ridgway (1997). The vertical coloured bar outlined in black is a representation of the CSEM model for the southern transmitter tow, shown in Fig. 3. Vertical exaggeration is 4:1.

high conductivity (in red) in this part of the model are probably a result of modest overfitting of the data and limitations of the 2-D bathymetry model, both in terms of detail and dimensionality.

The CSEM layered modelling for the southern transmitter tow provides an estimate of depth to electrical basement (i.e. 3.3 km), in good agreement with the gravity estimate (3.4 km). What is particularly intriguing is that both the gravity and the CSEM models require a small increase in resistivity and density at about 950 m deep in the sediments. This provides an interesting opportunity to remove one free variable in the binary mixing laws relating porosity and conductivity of pore fluids to rock conductivity.

If we assume a grain density of 2650 kg m^{-3} for the sediments (an average crustal value), then the porosities ϕ implied by the sediment densities are 0.33 (2100 kg m^{-3}) and 0.21 (2300 kg m^{-3}). If we next take Archie's Law to relate rock conductivity σ_r to porosity and pore fluid conductivity σ_f

$$\sigma_r = \sigma_f \phi^2 \tag{1}$$

then by taking sediment resistivities of 1.49 and 2.32 Ω-m from the CSEM models, we get pore fluid conductivities of 6.0 S m^{-1} for the upper sediments and 9.6 S m^{-1} for the lower sediments. The commonly used linear relationship between sea water conductivity and temperature T (in Celsius) of Becker *et al.* (1982)

$$\sigma_f = 3.0 + 0.1T \quad \text{S m}^{-1} \tag{2}$$

is only accurate to 3–5 per cent across the 0°–200°C temperature range. We can improve this by taking the cubic relationship of Perkin & Walker (1972) which is accurate over the 0°–25°C range and decreasing their coefficient of the cubic term by only 15 per cent to make the extrapolation match the 100°–200°C data of Quist & Marshall (1968), yielding

$$\sigma_f = 2.903916(1 + 0.0297175T + 0.00015551T^2 - 0.00000067T^3) \quad \text{S m}^{-1}. \tag{3}$$

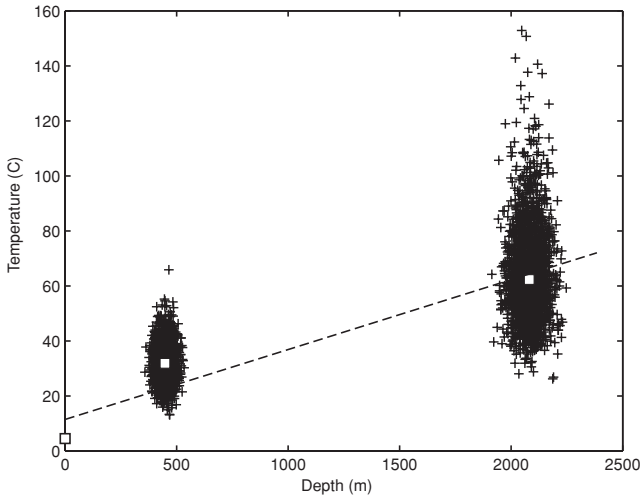

Figure 11. Temperature estimates obtained from computing porosity from density, pore fluid conductivity from porosity, and temperature from pore fluid conductivity (white-filled squares). The slope of the broken line is 25.4 K km^{-1}. The '+' symbols represent 2000 random perturbations around these temperature and depth estimates, allowing a standard deviation of 8 K km^{-1} to be estimated for the corresponding estimates of the geotherm.

Using this we infer temperatures of 31.8 and 62.5°C for the pore fluids, assuming they are of sea water salinity. If we assign the average depths of the two CSEM layers to these temperatures, and combine these with a temperature of 4.5°C logged near the seafloor by SUESI, we obtain an approximately linear relationship and a geothermal gradient of 25.4 K km^{-1} (Fig. 11). This is quite a reasonable value and, in a different environment, would be of use to an explorationist modelling the maturation history of hydrocarbons,

but it would be helpful to assign an uncertainty to this estimate. In an effort to assess the effect of uncertainty in the various numbers that went into this calculation, we ran a Monte Carlo simulation by adding zero-mean Gaussian perturbations to the densities, resistivities and depths. The three densities were perturbed with a standard deviation of 25 kg m^{-3}, the two resistivities by 5 per cent (which is about the variation seen in the Occam modelling) and the depths by 25 and 50 m, respectively. Two thousand realizations were generated and plotted in Fig. 11, yielding 2000 estimates of a geotherm g which are approximately normally distributed in $\sqrt{g}$. The average geotherm is 25.8 K km^{-1}, similar to the original estimate (as one would hope for zero-mean noise), and the standard deviation is about 8 K km^{-1}. The only remaining assumption is the salinity of the pore water, which for recently deposited marine sediments is likely close to sea water composition.

6 CONCLUSIONS

Although the current interest in marine electromagnetic methods is focused on the evaluation of hydrocarbon drilling targets (Eidesmo *et al.* 2002; Constable & Srnka 2007), the marine MT and the CSEM methods have great potential for mapping offshore sedimentary structure, especially if used in combination. The MT method in particular provides a relatively inexpensive reconnaissance tool for this purpose—the 10 sites presented here represent a modest investment of resources, yet provide fundamental information about geological structure. When EM data are combined with other geophysical data streams such as gravity and 2-D reflection seismics, a high degree of confidence in the geological interpretation is obtained. However, unlike CSEM, where the EM fields are primarily concentrated between source and receiver, MT fields are sensitive to bathymetry on local, regional, and at long periods even global scales. This makes accurate modelling of seafloor topography essential for the accurate interpretation of seafloor geology. Currently, this means that in a practical sense one is limited to 2-D geometries for terrain, geology and the coast effect.

ACKNOWLEDGMENTS

The authors would like to thank AGO (now WesternGeco Electromagnetics) for funding the development of the Mark III electromagnetic recorder, and ExxonMobil for funding the CSEM instrument trials. Additional funding from the Scripps Seafloor Electromagnetic Methods Consortium made this analysis possible. Jim Behrens did some preliminary processing of the CSEM data. Gary Egbert and Phil Wannamaker kindly made their codes available for community use. Jacques Lemire and the other technicians and engineers of the SIO Marine EM Laboratory built, maintained, and helped deploy the instruments used for this study. The staff of AGO assisted in the collection of the marine MT data. The SIO marine facility and the captains and crews of the R.V. New Horizon and R.V. Robert Gordon Sproul provided support for the marine operations. Paul Henkart assisted with processing seismic data. L.L. would like to thank George Jiracek for support during her Masters studies. Two anonymous reviewers and the Editor made suggestions which undoubtedly led to improvements in the manuscript. Copies of the data used in this paper can be obtained from http://marineemlab.ucsd.edu/Projects/Trough/

REFERENCES

Baba, K. & Chave, A.D., 2005. Correction of seafloor magnetotelluric data for topographic effects during inversion, *J. geophys. Res.,* **110,** Art. No. B12105, 1–16.

Baba, K. & Seama, N., 2002. New technique for the incorporation of seafloor topography in electromagnetic modelling, *Geophys. J. Int.,* **50,** 392–420.

Becker, K. *et al.*, 1982. *In situ* electrical resistivity and bulk porosity of the oceanic crust Costa Rica Rift, *Nature,* **300,** 594–598.

Constable, S., 2006. Marine electromagnetic methods-a new tool for offshore exploration, *Leading Edge,* **25,** 438–444.

Constable, S. & Cox, C.S., 1996. Marine controlled source electromagnetic sounding 2. The PEGASUS experiment, *J. geophys. Res.,* **101,** 5519–5530.

Constable, S. & Srnka, L.J., 2007. An introduction to marine controlled source electromagnetic methods for hydrocarbon exploration, *Geophysics,* **72,** WA3–WA12.

Constable, S. & Weiss, C.J., 2005. Mapping thin resistors (and hydrocarbons) with marine EM methods: insights from 1D modeling, *Geophysics,* **71,** G43–G51.

Constable, S.C., Parker, R.L. & Constable, C.G., 1987. Occam's Inversion: a practical algorithm for generating smooth models from EM sounding data, *Geophysics,* **52,** 289–300.

Constable, S., Orange, A., Hoversten, G.M. & Morrison, H.F., 1998. Marine magnetotellurics for petroleum exploration, part 1: a sea-floor instrument system, *Geophysics,* **63,** 816–825.

Cox, C., 1980. Electromagnetic induction in the oceans and inferences on the constitution of the earth, *Geophys. Surv.,* **4,** 137–156.

deGroot-Hedlin, C. & Constable, S.C., 1990. Occam's inversion to generate smooth, two-dimensional models from magnetotelluric data, *Geophysics,* **55,** 1613–1624.

deGroot-Hedlin, C. & Constable, S., 2004. Inversion of magnetotelluric data for 2D structure with sharp resistivity contrasts, *Geophysics,* **69,** 78–86.

Egbert, G.D., 1997. Robust multiple-station magnetotelluric data processing, *Geophys. J. Int.,* **130,** 475–496.

Eidesmo, T., Ellingsrud, S., MacGregor, L.M., Constable, S., Sinha, M.C., Johanson, S., Kong, F.N. & Westerdahl, H., 2002. Sea Bed Logging (SBL), a new method for remote and direct identification of hydrocarbon filled layers in deepwater areas, *First Break,* **20,** 144–152.

Filloux, J.H., 1979. Magnetotelluric and related electromagnetic investigations in geophysics, *Rev. Geophys. Space Phys.,* **17,** 282–294.

Fischer, G., 1979. Electromagnetic induction effects at an ocean coast, *Proc. IEEE,* **67,** 1050–1060.

Flosadottir, A.H. & Constable, S., 1996. Marine controlled source electromagnetic sounding 1. Modeling and experimental design, *J. geophys. Res.,* **101,** 5507–5517.

Gomez-Trevino, E. & Edwards, R.N., 1983. Electromagnetic soundings in the sedimentary basin of Southern Ontario-a case history, *Geophysics,* **48,** 311–330.

Heinson, G. & Constable, S.C., 1992. The electrical conductivity of the oceanic upper mantle, *Geophys. J. Int.,* **110,** 159–179.

Hördt, A., Jödicke, H., Strack, K.-M., Vozoff, K. & Wolfgram, P.A., 1992. Inversion of long-offset TEM soundings near the borehole Münsterland 1, Germany, and comparison with MT measurements, *Geophys. J. Int.,* **108,** 930–940.

Key, K., in press. One-dimensional inversion of mulit-component, multi-frequency marine CSEM data: methodology and synthetic studies for resolving thin resistive layers, *Geophysics*.

Key, K. & Weiss, C., 2006. Adaptive finite element modeling using unstructured grids: the 2D magnetotelluric example, *Geophysics,* **71,** G291–G299.

Legg, M.R. & Kamerling, M.J., 2003. Large-scale basement-involved landslides, California continental borderland, *Pure appl. Geophys.,* **160,** 2033–2051.

Lewis, L., 2005. A marine magnetotelluric study of the San Diego Trough Offshore California, USA, *Masters thesis*, San Diego State University.

Perkin, R.G. & Walker, E.R., 1972. Salinity calculations from in situ measurements, *J. geophys. Res.,* **77,** 6618–6621.

Quist, A.S. & Marshall, W.L., 1968. Electrical conductances of aqueous sodium chloride solutions from 0 to 800° and at pressures to 4000 Bars, *J. phys. Chem.,* **71,** 684–703.

Ranganayaki, R.P. & Madden, T.R., 1980. Generalized thin sheet analysis in magnetotellurics—an extension of Price analysis, *Geophys. J. R. astr. Soc.,* **60,** 445–457.

Ridgway, J.R., 1997. The development of a deep-towed gravity meter, and its use in marine geophysical surveys of offshore Southern California, and an Airborne Laser Altimeter Survey of Long Valley, California, *PhD thesis*, University of California, San Diego.

Ridgway, J.R. & Zumberge, M.A., 2002. Deep-towed gravity surveys in the southern California Continental Borderland, *Geophysics,* **67,** 777–787.

Schwalenberg, K. & Edwards, R.N., 2004. The effect of sea-floor topography on magnetotelluric fields: an analytic formulation confirmed with numerical results, *Geophys. J. Int.,* **159,** 607–621.

Shor, G.G. Jr., Raitt, R.W. & McGowan, D.D., 1976. *Seismic Refraction Studies in the Southern California Borderland, 1949-1974,* Scripps Inst. Ocean, Ref. 76–13.

Smith, T., Hoversten, M., Gasperikova, E. & Morrison, F., 1999. Sharp boundary inversion of 2D magnetotelluric data, *Geophys. Prospect.,* **47,** 469–486.

Swift, C.M.J., 1986. A magnetotelluric investigation of an electrical conductivity anomaly in the southwestern United States, in *Magnetotelluric Methods,* pp. 156–166, ed. Vozoff, K., Soc. Expl. Geophys.

Teng, L.S. & Gorsline, D.S., 1991. Stratigraphic framework of the continental borderland basins, southern California, in *The Gulf and Peninsular Province of the Californias,* Memoir 47, pp. 127–143, eds Dauplin, J.P. & Simone, B.R.T., AAPG.

Vozoff, K., 1972. The magnetotelluric method in the exploration of sedimentary basins, *Geophysics,* **37,** 98–141.

Wannamaker, P.E., Stodt, J.A. & Rijo, L., 1987. A stable finite-element solution for two-dimensional magnetotelluric modeling, *Geophys. J. R. astr. Soc.,* **88,** 277–296.

Webb, S.C., Constable, S.C., Cox, C.S. & Deaton, T.K., 1985. A sea-floor electric field instrument, *Geomag. Geoelectr.,* **37,** 1115–1129.